Continuous-time chaotic systems: Arbitrary full-state hybrid projective synchronization via a scalar signal

Giuseppe Grassi[†]

Dipartimento Ingegneria Innovazione, Università del Salento–73100 Lecce, Italy

(Received 4 December 2012; revised manuscript received 12 January 2013)

Referring to continuous-time chaotic systems, this paper presents a new projective synchronization scheme, which enables each drive system state to be synchronized with a linear combination of response system states for any arbitrary scaling matrix. The proposed method, based on a structural condition related to the uncontrollable eigenvalues of the error system, can be applied to a wide class of continuous-time chaotic (hyperchaotic) systems and represents a general framework that includes any type of synchronization defined to date. An example involving a hyperchaotic oscillator is reported, with the aim of showing how a response system attractor is arbitrarily shaped using a scalar synchronizing signal only. Finally, it is shown that the recently introduced dislocated synchronization can be readily achieved using the conceived scheme.

Keywords: continuous-time chaotic systems, chaos synchronization, observer-based synchronization, scalar synchronizing signal

PACS: 05.45.−a, 05.45.Xt **DOI:** 10.1088/1674-1056/22/8/080505

1. Introduction

Chaos synchronization is a fascinating topic in nonlinear science.[1] In fact, as chaos is characterized by a sensitive dependence on initial conditions, one could conclude that synchronization is not obtainable, since even infinitesimal change will eventually result in divergence of nearby starting orbits. Carroll and Pecora[2] were the first to prove that the dynamics of a drive system and of a driven subsystem (response system) become synchronized if the Lyapunov exponents of the response system are less than zero. With the passing of time several techniques for obtaining synchronized dynamics have been developed, including those focusing on the synchronization of hyperchaotic systems via a scalar synchronizing signal.[3–8] Besides the identical synchronization introduced by Carroll and Pecora, different types of synchronization have been successively developed.[9–18] For example, in projective synchronization[11–13] the response system states are scaled replicas of the drive system states. When the scaling factor equals −1, the projective synchronization turns into the anti-phase synchronization.[13] A variation of the projective synchronization is represented by the full-state hybrid projective synchronization,[14–17] where the scaling factor can be different for each state variable (i.e., the scaling matrix is a diagonal one). For example, in Refs. [14] and [15] an active control scheme is utilized to achieve the full-state hybrid projective synchronization in some hyperchaotic continuous-time systems, whereas in Ref. [16] the active control is adopted to synchronize a class of chaotic maps. Moreover, in Ref. [17] the Lyapunov stability theory is utilized to achieve the full-state hybrid projective synchronization for a new chaotic system. Even though the approaches in Refs. [14]–[17] are interesting, they present the drawback that synchronization is achieved using several control signals, while communications based on projective synchronization require a scalar synchronizing signal.[18] Very recently, the full-state hybrid projective synchronization has been generalized by considering an arbitrary scaling matrix, instead of a diagonal one.[18] The approach, which has been called arbitrary full-state hybrid projective synchronization[18] (AFSHPS), enables each drive system state to be synchronized with a linear combination of response system states. However, the method in Ref. [18] has been developed for discrete-time systems only, i.e., an approach involving the AFSHPS for continuous-time systems is still lacking. Based on these considerations, this paper aims to bridge the gap by introducing a technique to achieve the AFSHPS for a wide class of continuous-time systems. Moreover, the proposed synchronization approach is based on a structural condition related to the uncontrollable eigenvalues of the error system, which is less restrictive with respect to the controllability condition reported in Ref. [18].

The rest of the present paper is organized as follows. Section 2 illustrates two propositions that enable each drive system variable to be synchronized with any linear combination of response system variables. A remarkable feature of the proposed scheme is that synchronization is achievable via a scalar signal for a wide class of continuous-time systems, which include several well-known chaotic and hyperchaotic systems. Section 3 illustrates the advantages of the method, including the fact that it represents a general framework for obtaining any type of synchronization defined to date. Sec-

[†]Corresponding author. E-mail: giuseppe.grassi@unisalento.it

© 2013 Chinese Physical Society and IOP Publishing Ltd

tion 4 presents an example, involving the hyperchaotic oscillator implemented by the author in Ref. [8], which clearly shows how the AFSHPS can be effectively achieved. Moreover, the reported plots highlight that by virtue of the considered arbitrary scaling matrix, the response system attractor is arbitrarily shaped by the scalar signal generated by the drive system. Finally, the example shows that the dislocated synchronization recently presented in Ref. [19] can be readily achieved using the conceived synchronization scheme.

2. Continuous-time systems: Arbitrary full-state hybrid projective synchronization

This work focuses on the class of drive systems defined by the following continuous-time state and output equations, respectively:

$$\dot{\boldsymbol{x}}(t) = \boldsymbol{A}\boldsymbol{x}(t) + \boldsymbol{b}f(\boldsymbol{x}(t)) + \boldsymbol{c}, \tag{1}$$

$$y(t) = f(\boldsymbol{x}(t)) + \boldsymbol{k}\boldsymbol{x}(t), \tag{2}$$

where $x(t) \in \Re^{n\times 1}$ is the state vector, $\boldsymbol{A} \in \Re^{n\times n}$, $\boldsymbol{b} \in \Re^{n\times 1}$, and $\boldsymbol{c} \in \Re^{n\times 1}$ are constant matrices, $f : \Re^n \to \Re$ is a scalar nonlinear function, $y(t)$ is a scalar synchronizing output and $\boldsymbol{k} \in \Re^{1\times n}$ is a gain vector to be determined. As pointed out in Refs. [5]–[7], the class described by Eq. (1) includes several well-known chaotic (hyperchaotic) systems characterized by one nonlinear term. Examples of these systems include Chua's circuit, Rössler's system, the Matsumoto–Chua–Kobayashi circuit and the higher-dimensional Chua's circuit. The class (1) also includes the hyperchaotic oscillator implemented by the author in Ref. [8] and the circuit for generating multi-scrolls described in Ref. [20].

Now, by taking into account the definition reported in Ref. [18] for discrete-time systems, the arbitrary full-state hybrid projective synchronization (AFSHPS) for continuous-time systems is introduced. Namely, the drive system (1) and the n-dimensional state vector $\hat{\boldsymbol{x}}(t)$, describing the response system dynamics, are said to be in AFSHPS when each drive system variable $x_i(t)$ synchronizes with a linear combination of response system variables $(\alpha_{i1}\hat{x}_1(t) + \alpha_{i2}\hat{x}_2(t) + \cdots \alpha_{in}\hat{x}_n(t))$, i.e.,

$$\|e_i(t)\| = \left\| (x_i(t) - \sum_{j=1}^{n} \alpha_{ij}\hat{x}_j(t)) \right\| \to 0 \quad \text{as} \quad t \to \infty, \quad i = 1,2,\ldots,n, \tag{3}$$

where α_{ij} $(i = 1,2,\ldots,n,\ j = 1,2,\ldots,n)$ represent the elements of the arbitrary scaling matrix and, consequently, the weights of the linear combination in Eq. (3).

Given the drive system (1), the observed-based approach[5] enables the state $\boldsymbol{x}(t)$ to be reconstructed by a response system (described by state vector $\hat{\boldsymbol{x}}(t)$) via a scalar function of the states $y(t)$ and its prediction $\hat{y}(t)$. Note that the response system need not be a copy of the drive system in order to obtain synchronized dynamics.[6] Thus, the following proposition is given, with the aim of obtaining the error dynamics between drive and response systems.

Proposition 1 Given the drive systems (1) and (2), let

$$\dot{\hat{\boldsymbol{x}}}(t) = \boldsymbol{\alpha}^{-1}\boldsymbol{A}\boldsymbol{\alpha}\hat{\boldsymbol{x}}(t) + \boldsymbol{\alpha}^{-1}\boldsymbol{b}f(\hat{\boldsymbol{x}}(t)) + \boldsymbol{\alpha}^{-1}\boldsymbol{c} + \boldsymbol{\alpha}^{-1}\boldsymbol{b}(y(t) - \hat{y}(t)), \tag{4}$$

$$\hat{y}(t) = f(\hat{\boldsymbol{x}}(t)) + \boldsymbol{k}\boldsymbol{\alpha}\hat{\boldsymbol{x}}(t) \tag{5}$$

be the response system in the observer form, where

$$\boldsymbol{\alpha} = \begin{bmatrix} \alpha_{11} & \alpha_{12} & \ldots & \alpha_{1n} \\ \alpha_{21} & \alpha_{22} & \ldots & \alpha_{2n} \\ \ldots & \ldots & \ldots & \ldots \\ \alpha_{n1} & \alpha_{n2} & \ldots & \alpha_{nn} \end{bmatrix} \tag{6}$$

is the n-th order scaling matrix derived from the system (3). Then the error dynamics between the drive systems (1) and (2) and the response systems (4) and (5) is linear time-invariant and can be expressed as

$$\dot{\boldsymbol{e}}(t) = \boldsymbol{A}\boldsymbol{e}(t) - \boldsymbol{b}\boldsymbol{k}\boldsymbol{e}(t) = \boldsymbol{A}\boldsymbol{e}(t) + \boldsymbol{b}\boldsymbol{u}(t), \tag{7}$$

where $u(t) = -\boldsymbol{k}\boldsymbol{e}(t)$ plays the role of a state feedback.

Proof By exploiting expression (6), the error (3) can be written in a matrix form as

$$\|\boldsymbol{e}(t)\| = \|(\boldsymbol{x}(t) - \boldsymbol{\alpha}\hat{\boldsymbol{x}}(t))\|. \tag{8}$$

By taking into account systems (1), (2) and (4), (5), it follows that

$$\begin{aligned} \dot{\boldsymbol{e}}(t) &= (\dot{\boldsymbol{x}}(t) - \boldsymbol{\alpha}\dot{\hat{\boldsymbol{x}}}(t)) \\ &= \boldsymbol{A}\boldsymbol{x}(t) + \boldsymbol{b}f(\boldsymbol{x}(t)) + \boldsymbol{c} - \boldsymbol{A}\boldsymbol{\alpha}\hat{\boldsymbol{x}}(t) - \boldsymbol{b}f(\hat{\boldsymbol{x}}(t)) \\ &\quad - \boldsymbol{c} - \boldsymbol{b}(y(t) - \hat{y}(t)) \\ &= \boldsymbol{A}(\boldsymbol{x}(t) - \boldsymbol{\alpha}\hat{\boldsymbol{x}}(t)) + \boldsymbol{b}f(\boldsymbol{x}(t)) - \boldsymbol{b}f(\hat{\boldsymbol{x}}(t)) - \boldsymbol{b}(f(\boldsymbol{x}(t)) \\ &\quad + \boldsymbol{k}\boldsymbol{x}(t) - f(\hat{\boldsymbol{x}}(t)) - \boldsymbol{k}\boldsymbol{\alpha}\hat{\boldsymbol{x}}(t)) \\ &= \boldsymbol{A}(\boldsymbol{x}(t) - \boldsymbol{\alpha}\hat{\boldsymbol{x}}(t)) - \boldsymbol{b}\boldsymbol{k}(\boldsymbol{x}(t) - \boldsymbol{\alpha}\hat{\boldsymbol{x}}(t)) \\ &= \boldsymbol{A}\boldsymbol{e}(t) - \boldsymbol{b}\boldsymbol{k}\boldsymbol{e}(t). \end{aligned} \tag{9}$$

Thus, the error dynamics is described by the linear time invariant system $\dot{\boldsymbol{e}}(t) = \boldsymbol{A}\boldsymbol{e}(t) + \boldsymbol{b}\boldsymbol{u}(t)$, where $u(t) = -\boldsymbol{k}\boldsymbol{e}(t)$.

In order to synchronize the drive systems (1) and (2) with the response systems (4) and (5), it is necessary to properly compute the gain vector $\boldsymbol{k} \in \Re^{1\times n}$. For this purpose, the following proposition is now given.

Proposition 2 The response systems (4) and (5) and the drive systems (1) and (2) achieve AFSHPS for any $\hat{x}(0)$, provided that all the uncontrollable eigenvalues of the error system (7), if any, have negative real parts.

Proof For system (7) a coordinate transformation $\boldsymbol{e} = [\,\boldsymbol{T}_1\ \boldsymbol{T}_2\,]\bar{\boldsymbol{e}}$ can be found,[5] where the columns of $\boldsymbol{T}_1$ and $\boldsymbol{T}_2$ generate the controllable-state subspace and the uncontrollable-state subspace, respectively. By defining $\bar{\boldsymbol{A}}_c = \boldsymbol{T}_1^{\mathrm{T}}\boldsymbol{A}\boldsymbol{T}_1$, $\bar{\boldsymbol{A}}_{12} = \boldsymbol{T}_1^{\mathrm{T}}\boldsymbol{A}\boldsymbol{T}_2$, $\bar{\boldsymbol{A}}_{nc} = \boldsymbol{T}_2^{\mathrm{T}}\boldsymbol{A}\boldsymbol{T}_2$, and $\bar{\boldsymbol{b}}_c = \boldsymbol{T}_1^{\mathrm{T}}\boldsymbol{b}$, system (7) can be transformed to the Kalman controllable canon-

ical form[5] as follows:

$$\begin{bmatrix} \dot{\bar{e}}_c(t) \\ \dot{\bar{e}}_{nc}(t) \end{bmatrix} = \begin{bmatrix} \bar{A}_c & \bar{A}_{12} \\ 0 & \bar{A}_{nc} \end{bmatrix} \begin{bmatrix} \bar{e}_c(t) \\ \bar{e}_{nc}(t) \end{bmatrix} + \begin{bmatrix} \bar{b}_c \\ 0 \end{bmatrix} u(t), \quad (10)$$

where the eigenvalues of $\bar{A}_c$ are controllable, i.e., they can be placed anywhere by state feedback $u(t) = -ke(t)$, whereas the eigenvalues of $\bar{A}_{nc}$ are uncontrollable, i.e., they are not affected by the introduction of any state feedback. Therefore, system (7) can be globally asymptotically stabilized by suitable k, provided that the eigenvalues of $\bar{A}_{nc}$ lie in the left half plane.[21–23] Since $\|\bar{e}(t)\| \to 0$ implies $\|e(t)\| \to 0$, this means that the response system (4) and the drive system (1) achieve the AFSHPS for any initial condition $\hat{x}(0)$ and for any weight matrix α via the scalar synchronizing signal (2).

3. Advantages of the synchronization scheme

As pointed out in Section 2, the class described by system (1) includes Chua's circuit, Rössler's system, the Matsumoto–Chua–Kobayashi circuit, the higher dimensional Chua's circuit, the hyperchaotic oscillator illustrated in Ref. [8], and the circuit for generating multi-scrolls described in Ref. [20]. By considering, for each of these systems, the matrices A and b in system (1), and by computing the matrices

$$\begin{bmatrix} \bar{A}_c & \bar{A}_{12} \\ 0 & \bar{A}_{nc} \end{bmatrix}, \quad (11)$$

it can be readily shown that $\bar{A}_{nc}$ is the null matrix for each of these systems. As a consequence, the eigenvalues of the error system (10) are all controllable, i.e., they can be placed anywhere by suitable k. This clearly indicates that the proposed synchronization scheme can be successfully applied to a wide class of chaotic systems characterized by one nonlinear term.

Another advantage is that the proposed scheme represents a general framework to achieve any type of synchronization defined so far. Namely, when $\alpha_{11} = \alpha_{22} = \cdots = \alpha_{nn} = 1$ and $\alpha_{ij} = 0$, $i \neq j$, identical (complete) synchronization is achieved, whereas for $\alpha_{11} = \alpha_{22} = \cdots = \alpha_{nn} = -1$ and $\alpha_{ij} = 0$, $i \neq j$, anti-phase synchronization is obtained. Moreover, when $\alpha_{11} = \alpha_{22} = \cdots = \alpha_{nn} = \alpha$ and $\alpha_{ij} = 0$, $i \neq j$, the projective synchronization as proposed in Refs. [11]–[13] is obtained. On the other hand, when $\alpha_{11} \neq \alpha_{22} \neq \cdots \neq \alpha_{nn}$ and $\alpha_{ij} = 0$, $i \neq j$, the full-state hybrid projective synchronization as defined in Refs. [14]–[17] is obtained, whereas for $\alpha_{11} = \alpha_{22} = \cdots = \alpha_{nn} = 0$ and $\alpha_{ij} \neq 0$, $i \neq j$ the dislocated synchronization is achieved.[19]

Other advantages of the proposed observer-based scheme are the following.

(i) It represents a rigorous and systematic approach to synchronization (being the method based on two propositions);

(ii) It does not require computation of Lyapunov exponents in order to check synchronization;

(iii) It can be implemented in hardware as shown by the author of the present paper in Ref. [8], where a similar continuous-time observer, though without a scaling ability, has been successfully implemented (indicating that the observer-based method is able to be electronically realized).

4. Examples: AFSHPS and dislocated synchronization

The aim of this section is to illustrate, via practical examples, both the AFSHPS proposed herein and the dislocated synchronization recently developed in Ref. [19]. In particular, referring to the AFSHPS, the reported plots highlight that the response system attractor is arbitrarily shaped by the scalar signal generated by the drive system.

4.1. Arbitrary full-state hybrid projective synchronization

The drive system considered herein is the hyperchaotic oscillator implemented by the author in Ref. [8]. It mainly contains two LC circuits and a diode.[7,8] The oscillator dynamics can be written in the form of system (1) as

$$\begin{bmatrix} \dot{x}_1(t) \\ \dot{x}_2(t) \\ \dot{x}_3(t) \\ \dot{x}_4(t) \end{bmatrix} = \begin{bmatrix} 0.7 & -1 & -1 & 0 \\ 1 & 0 & 0 & 0 \\ 3 & 0 & 0 & -3 \\ 0 & 0 & 3 & 0 \end{bmatrix} \begin{bmatrix} x_1(t) \\ x_2(t) \\ x_3(t) \\ x_4(t) \end{bmatrix} + \begin{bmatrix} 0 \\ 0 \\ 0 \\ -30 \end{bmatrix} (x_4(t) - 1)H(x_4(t) - 1), \quad (12)$$

where $H(z)$ is the Heaviside function describing the diode behavior (i.e., $H(z < 0) = 0$ and $H(z \geq 0) = 1$). Given the matrices A and b in Eq. (12), it can be readily shown that $\bar{A}_{nc}$ is the null matrix. As a consequence, all the eigenvalues of the error system (10) are controllable, i.e., they can be placed anywhere by suitable k. Taking the eigenvalues to be -1 leads to $k = [\,-47.49 \;\; -104.17 \;\; 6.83 \;\; -1.35\,]$. Thus, the output of system (12) becomes the scalar synchronizing signal

$$\begin{aligned} y(t) \;=\; & (x_4(t) - 1)H(x_4(t) - 1) \\ & + [\,-47.49 \;\; -104.17 \;\; 6.83 \;\; -1.35\,] \\ & \times [\,x_1(t) \;\; x_2(t) \;\; x_3(t) \;\; x_4(t)\,]^{\mathrm{T}}, \end{aligned} \quad (13)$$

whereas the dynamics of the observer (4) are described by

$$\begin{bmatrix} \dot{\hat{x}}_1(t) \\ \dot{\hat{x}}_2(t) \\ \dot{\hat{x}}_3(t) \\ \dot{\hat{x}}_4(t) \end{bmatrix} = \begin{bmatrix} \alpha_{11} & \alpha_{12} & \alpha_{13} & \alpha_{14} \\ \alpha_{21} & \alpha_{22} & \alpha_{23} & \alpha_{24} \\ \alpha_{31} & \alpha_{32} & \alpha_{33} & \alpha_{34} \\ \alpha_{41} & \alpha_{42} & \alpha_{43} & \alpha_{44} \end{bmatrix}^{-1} \begin{bmatrix} 0.7 & -1 & -1 & 0 \\ 1 & 0 & 0 & 0 \\ 3 & 0 & 0 & -3 \\ 0 & 0 & 3 & 0 \end{bmatrix} \times \begin{bmatrix} \alpha_{11} & \alpha_{12} & \alpha_{13} & \alpha_{14} \\ \alpha_{21} & \alpha_{22} & \alpha_{23} & \alpha_{24} \\ \alpha_{31} & \alpha_{32} & \alpha_{33} & \alpha_{34} \\ \alpha_{41} & \alpha_{42} & \alpha_{43} & \alpha_{44} \end{bmatrix} \begin{bmatrix} \hat{x}_1(t) \\ \hat{x}_2(t) \\ \hat{x}_3(t) \\ \hat{x}_4(t) \end{bmatrix}$$

$$+\begin{bmatrix}\alpha_{11} & \alpha_{12} & \alpha_{13} & \alpha_{14}\\ \alpha_{21} & \alpha_{22} & \alpha_{23} & \alpha_{24}\\ \alpha_{31} & \alpha_{32} & \alpha_{33} & \alpha_{34}\\ \alpha_{41} & \alpha_{42} & \alpha_{43} & \alpha_{44}\end{bmatrix}^{-1}\begin{bmatrix}0\\0\\0\\-30\end{bmatrix}$$
$$\times(\hat{x}_4(t)-1)H(\hat{x}_4(t)-1)$$
$$+\begin{bmatrix}\alpha_{11} & \alpha_{12} & \alpha_{13} & \alpha_{14}\\ \alpha_{21} & \alpha_{22} & \alpha_{23} & \alpha_{24}\\ \alpha_{31} & \alpha_{32} & \alpha_{33} & \alpha_{34}\\ \alpha_{41} & \alpha_{42} & \alpha_{43} & \alpha_{44}\end{bmatrix}^{-1}\begin{bmatrix}0\\0\\0\\-30\end{bmatrix}$$
$$\times(y(t)-\hat{y}(t)), \tag{14}$$

$$\hat{y}(t)=\begin{bmatrix}-47.49 & -104.17 & 6.83 & -1.35\end{bmatrix}$$
$$\times\begin{bmatrix}\alpha_{11} & \alpha_{12} & \alpha_{13} & \alpha_{14}\\ \alpha_{21} & \alpha_{22} & \alpha_{23} & \alpha_{24}\\ \alpha_{31} & \alpha_{32} & \alpha_{33} & \alpha_{34}\\ \alpha_{41} & \alpha_{42} & \alpha_{43} & \alpha_{44}\end{bmatrix}\begin{bmatrix}\hat{x}_1(t)\\ \hat{x}_2(t)\\ \hat{x}_3(t)\\ \hat{x}_4(t)\end{bmatrix}$$
$$+(\hat{x}_4(t)-1)H(\hat{x}_4(t)-1), \tag{15}$$

where expression (15) is the observer prediction of the output (13). By virtue of Proposition 2, the response system (14) and the drive system (12) are in AFSHPS for any scaling matrix (6) via the scalar synchronizing signal (13).

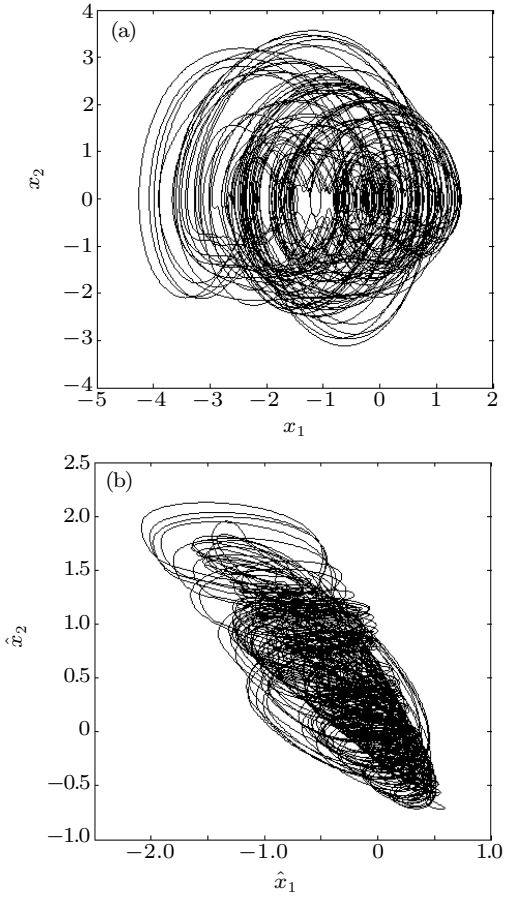


Fig. 1. Attractor of the drive system (12) in the (x_1,x_2)-plane (a) and attractor of the response system (14) in the $(\hat{x}_1,\hat{x}_2)$-plane (b). The scaling matrix is given in expression (16). Note that the shapes of the attractors in the two plots are completely different.

In order to show the effectiveness of the approach, simulations are carried out by choosing the following scaling matrix:

$$\boldsymbol{\alpha}=\begin{bmatrix}4 & 3 & 0 & 5\\ 0 & -2 & 0 & 0\\ 0 & 6 & -5 & -3\\ 0 & 0 & 0 & 7\end{bmatrix}. \tag{16}$$

Figure 1 shows the attractor of the drive system (12) in the (x_1,x_2)-plane (a) and the attractor of the response system (14) in the $(\hat{x}_1,\hat{x}_2)$-plane (b). These plots clearly highlight that the response system attractor has been arbitrarily shaped by the scalar signal (13) coming from the drive system (12). Namely, the variable $x_1(t)$ is synchronized with the linear combination of response system variables given by $4\hat{x}_1(t)+3\hat{x}_2(t)+5\hat{x}_4(t)$, whereas the variable $x_2(t)$ is synchronized with $-2\hat{x}_2(t)$. This generates in the $(\hat{x}_1,\hat{x}_2)$-plane an attractor characterized by a shape, which is completely different from the drive system attractor.

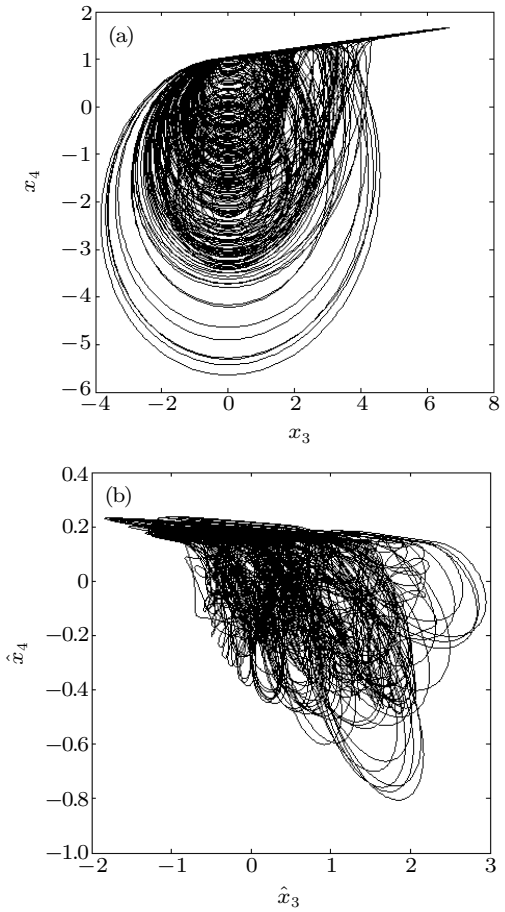


Fig. 2. Attractor of the drive system (12) in the (x_3,x_4)-plane (a) and attractor of the response system (14) in the $(\hat{x}_3,\hat{x}_4)$-plane (b). The scaling matrix is given in expression (16). Note that the shapes of the attractors in the two plots are completely different.

Additionally, figure 2 depicts the attractor of the drive system (12) in the (x_3,x_4)-plane (a) and the attractor of the response system (14) in the $(\hat{x}_3,\hat{x}_4)$-plane (b). According to expression (16), the variable $x_3(t)$ is synchronized with the linear combination of response system variables given by

$6\hat{x}_2(t)-5\hat{x}_3(t)-3\hat{x}_4(t)$, whereas the variable $x_4(t)$ is synchronized with $7\hat{x}_4(t)$. Clearly, the shape of the response system attractor in the $(\hat{x}_3,\hat{x}_4)$-plane is completely different from the shape of the drive system attractor in the (x_3,x_4)-plane, although the two systems achieve synchronized dynamics via the scalar signal (13).

Finally, the time behaviors of the synchronization errors as defined in expression (3), are reported in Fig. 3. The plots clearly show that the synchronization errors asymptotically go to zero, indicating that AFSHPS is achieved between systems (12) and (14).

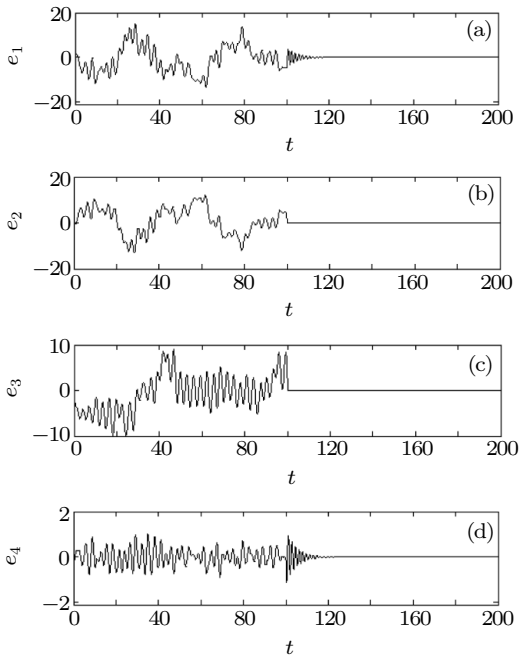


Fig. 3. Time behaviors of the synchronization errors: (a) $e_1(t) = x_1(t) - (4\hat{x}_1(t) + 3\hat{x}_2(t) + 5\hat{x}_4(t))$; (b) $e_2(t) = x_2(t) - (-2\hat{x}_2(t))$; (c) $e_3(t) = x_3(t) - (6\hat{x}_2(t) - 5\hat{x}_3(t) - 3\hat{x}_4(t))$; (d) $e_4(t) = x_4(t) - (7\hat{x}_4(t))$. The synchronizing signal (13) is switched on at $t = 100$. Note that the synchronization errors asymptotically go to zero, indicating that AFSHPS is achieved between systems (12) and (14).

5. Dislocated synchronization

Now an example of dislocated synchronization[19] is shown. According to this type of synchronization, the scaling factors must satisfy the condition $\alpha_{11} = \alpha_{22} = \cdots = \alpha_{nn} = 0$ and $\alpha_{ij} \neq 0$ when $i \neq j$ (see Ref. [19]). Simulations are carried out by considering the drive systems (12) and (13) and by taking the response systems (14) and (15) with the following scaling matrix:

$$\boldsymbol{\alpha} = \begin{bmatrix} 0 & 2 & 0 & 3 \\ 4 & 0 & 0 & 0 \\ 0 & 5 & 0 & 0 \\ -2 & -4 & -6 & 0 \end{bmatrix}. \tag{17}$$

According to the dislocated synchronization as defined in Ref. [19], the variables $x_1(t)$ and $x_3(t)$ are allowed to synchronize with all the response system variables except $\hat{x}_1(t)$ and $\hat{x}_3(t)$, respectively. In this case, $x_1(t)$ is synchronized with the linear combination of response system variables $2\hat{x}_2(t) + 3\hat{x}_4(t)$, whereas the variable $x_3(t)$ is synchronized with $5\hat{x}_2(t)$. Figure 4 shows the drive system attractor in the (x_1,x_3)-plane (a) and the response system attractor in the $(\hat{x}_1,\hat{x}_3)$-plane (b).

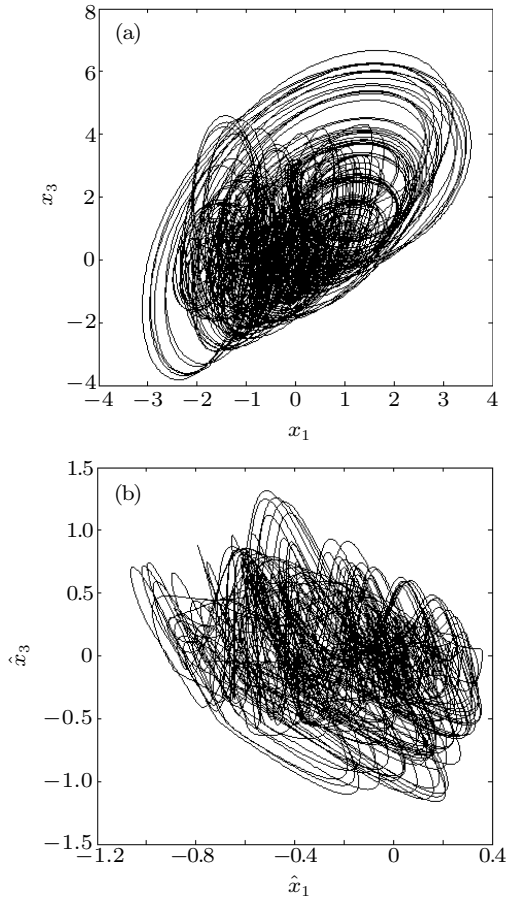


Fig. 4. Drive system attractor in the (x_1,x_3)-plane (a) and response system attractor in the $(\hat{x}_1,\hat{x}_3)$-plane (b). According to the dislocated synchronization, the variables $x_1(t)$ and $x_3(t)$ are allowed to synchronize with all the response system variables except $\hat{x}_1(t)$ and $\hat{x}_3(t)$, respectively.

Additionally, figure 5 depicts the attractor of the drive system (12) in the (x_2,x_4)-plane (a) and the attractor of the response system (14) in the $(\hat{x}_2,\hat{x}_4)$-plane (b). According to the scaling matrix (17), the variable $x_2(t)$ is synchronized with the response system variable $4\hat{x}_1(t)$, whereas the variable $x_4(t)$ is synchronized with the linear combination of response system variables $-2\hat{x}_1(t) - 4\hat{x}_2(t) - 6\hat{x}_3(t)$. Given that $x_2(t)$ and $x_4(t)$ do not synchronize with the response system variables $\hat{x}_2(t)$ and $\hat{x}_4(t)$, respectively, this confirms that dislocated synchronization is achieved between the drive system (12) and the response system (14).

Finally, the time behaviors of selected synchronization errors are reported in Fig. 6. As proved in Proposition 2, the errors asymptotically go to zero, indicating the effectiveness of the approach developed herein.

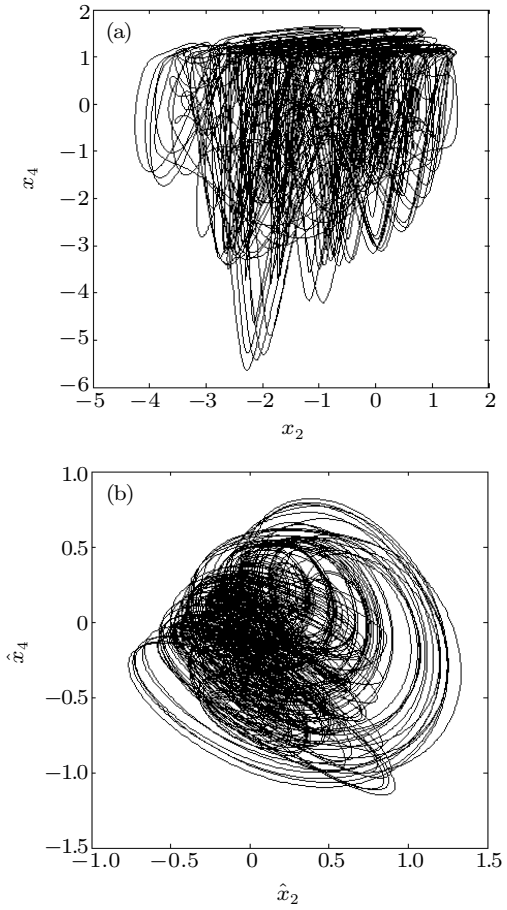


Fig. 5. Drive system attractor in the (x_2, x_4)-plane (a) and response system attractor in the $(\hat{x}_2, \hat{x}_4)$-plane (b). According to the dislocated synchronization, the variables $x_2(t)$ and $x_4(t)$ are allowed to synchronize with all the response system variables except $\hat{x}_2(t)$ and $\hat{x}_4(t)$, respectively.

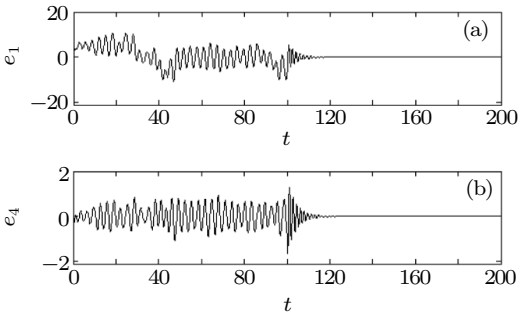


Fig. 6. Time behaviors of selected synchronization errors. (a): $e_1(t) = x_1(t) - (2\hat{x}_2(t) + 3\hat{x}_4(t))$; (b): $e_4(t) = x_4(t) - (-2\hat{x}_1(t) - 4\hat{x}_2(t) - 6\hat{x}_3(t))$. The synchronizing signal is switched on at $t = 100$. The errors $e_2(t)$ and $e_3(t)$ asymptotically go to zero in a similar way.

6. Conclusion

Referring to continuous-time chaotic systems, in this paper a new synchronization approach is introduced that enables a linear combination of response system variables to be synchronized with a drive system variable. The method, which features an observer with an ability to arbitrarily shape its attractor via a scalar synchronizing signal, is based on a structural condition related to the uncontrollable eigenvalues of the error system. In order to highlight the effectiveness of the technique, a numerical example is reported, which includes the dislocated synchronization as a particular case of the conceived scheme. To the best of the author's knowledge, the method developed herein is the only one to simultaneously include the following remarkable features regarding the synchronization of continuous-time systems: i) it represents a general framework that includes any type of synchronization defined to date; ii) synchronization is achieved using a scalar signal only; iii) it is rigorous (being based on two propositions); and iv) it can be applied in a systematic way to a wide class of chaotic (hyperchaotic) systems. In conclusion, the author feels that the present work for continuous-time systems and the companion paper[18] for discrete-time systems may represent a unified framework for achieving any type of chaos synchronization defined to date, for most of the continuous- and discrete-time systems developed to date.

References

[1] Li Y and Liu Z R 2010 *Chin. Phys. B* **19** 110501
[2] Carroll T L and Pecora L M 1991 *IEEE Trans. Circ. Sys.* **38** 453
[3] Grassi G and Mascolo S 1999 *IEEE Trans. Circ. Sys.* **I46** 1135
[4] Grassi G and Mascolo S 1999 *Int. J. Circ. Theory Appl.* **27** 543
[5] Grassi G and Mascolo S 1997 *IEEE Trans. Circ. Sys.* **I44** 1011
[6] Grassi G and S. Mascolo 1999 *IEEE Trans. Circ. Sys.* **II46** 478
[7] Grassi G and Mascolo S 1998 *IEE Electron. Lett.* **34** 424
[8] Miller D A and Grassi G 2001 *IEEE Trans. Circ. Sys.* **I48** 366
[9] Brucoli, M, Carnimeo L and Grassi G 1996 *Int. J. Bifur. Chaos* **6** 1673
[10] Brucoli, M, Carnimeo L and Grassi G 1996 *Int. J. Circ. Theory Appl.* **24** 489
[11] Mainieri R and Rehacek J 1999 *Phys. Rev. Lett.* **82** 3042
[12] Grassi G and Miller D A 2009 *Chaos, Solitons & Fractals* **39** 1246
[13] Grassi G and Miller D A 2007 *Int. J. Bifur. Chaos* **17** 1337
[14] Hu M, Xu Z, Zhang R and Hu A 2007 *Phys. Lett. A* **361** 231
[15] Hu M, Xu Z and Zhang R 2008 *Commun. Nonlinear Sci. Numer. Simul.* **13** 456
[16] Hu M, Xu Z and Zhang R 2008 *Commun. Nonlinear Sci. Numer. Simul.* **13** 782
[17] Dai H, Jia L X, Hui M and Si G Q 2011 *Chin. Phys. B* **20** 040507
[18] Grassi G 2012 *Chin. Phys. B* **21** 060504
[19] Chu Y D, Chang Y X, An X L, Yu J N and Zhang J G 2011 *Commun. Nonlinear Sci. Numer. Simul.* **16** 1509
[20] Tang W K S, Zhong G Q, Chen G and Man K F 2001 *IEEE Trans. Circ. Sys.* **I48** 1369
[21] Grassi G and Vecchio P 2007 *Dynamics of Continuous, Discrete and Impulsive Systems B* **14** 705
[22] Grassi G and Grieco LA 2003 *IEEE Trans. Circ. Sys.* **I50** 488
[23] Guo L X, Xu Z Y and Hu M F 2008 *Chin. Phys. B* **17** 4067